

## 5.2. Palmer Station (7/23/01 – 7/9/02)

The 2001-2002 season at Palmer Station is defined as the time between the season opening system service, performed between 07/14/01 - 07/23/01, and the site visit in 2002, which took place between 7/9/02 and 7/17/02. Note that there is no solar data available for the period 5/18/01 (end of Volume 10) and 7/22/01. The instrument service in 2001 was performed by the system operator at Palmer station and took longer than expected due to his involvement in other projects. Season opening absolute calibrations were performed between 7/19/01 and 7/21/01; season closing calibrations were carried out on 7/10/02. Volume 11 solar data comprise the period 7/23/01 – 7/9/02.

In general, the system performed as expected. About 96% of the scheduled data scans are part of the published dataset; 3% of all scans were lost as the monochromator offset became misadjusted four times in 2001. Affected scans had to be discarded.

During both site visits, the Eppley PSP and TUVR instruments were replaced by identical instruments, which had been calibrated by Eppley before the site visit. The previously installed instruments were sent to the manufacturer for recalibration.

### 5.2.1. Irradiance Calibration

The site irradiance standards for 2001-2002 were the lamps 200W007, M-765, and M-700. Lamp M-764 was used as the traveling standard both at the beginning and end of the season. In addition lamp 200W017 was used during season opening calibrations.

Lamp 200W007 has an irradiance calibration from Optronic Laboratories from November 1996. Lamp M-765 has an Optronic Laboratories calibration from 1992 and has been in use at Palmer Station since 1992. The lamp was recalibrated with the previous traveling standard M-874 using data from the Volume 9 opening calibrations. Lamp M-700 was calibrated in a similar fashion as lamp M-765; the irradiance calibration was transferred from the traveling standard M-874 using absolute scans of both lamps from days 5/11/99 and 5/12/99. The calibrations of all three site standards was the same as in Volume 10. The traveling standard M-764 and lamp 200W017 were calibrated by Optronic Laboratories in March 2001.

Figure 5.2.1 shows the Volume 11 season opening calibrations. All site standards and lamp 200W017 agree on the  $\pm 1\%$  level, but there is a bias of 1-2% compared to the calibration of the traveling standard M-764. Figure 5.2.2 shows the Volume 11 season closing calibrations performed on 7/10/02. All lamps agree with M-764 to within  $\pm 1.5\%$ . The result is very consistent to the season opening calibrations.

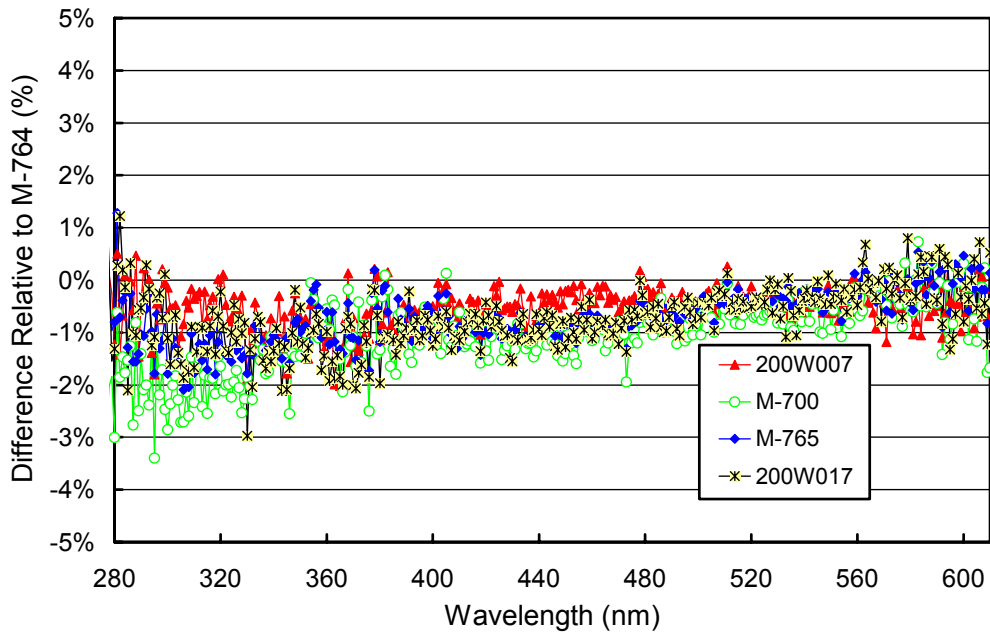


**Figure 5.2.1.** Comparison of Palmer lamps 200W007, M-700, and M-765 with the BSI traveling standard M-764 at the beginning of the season.

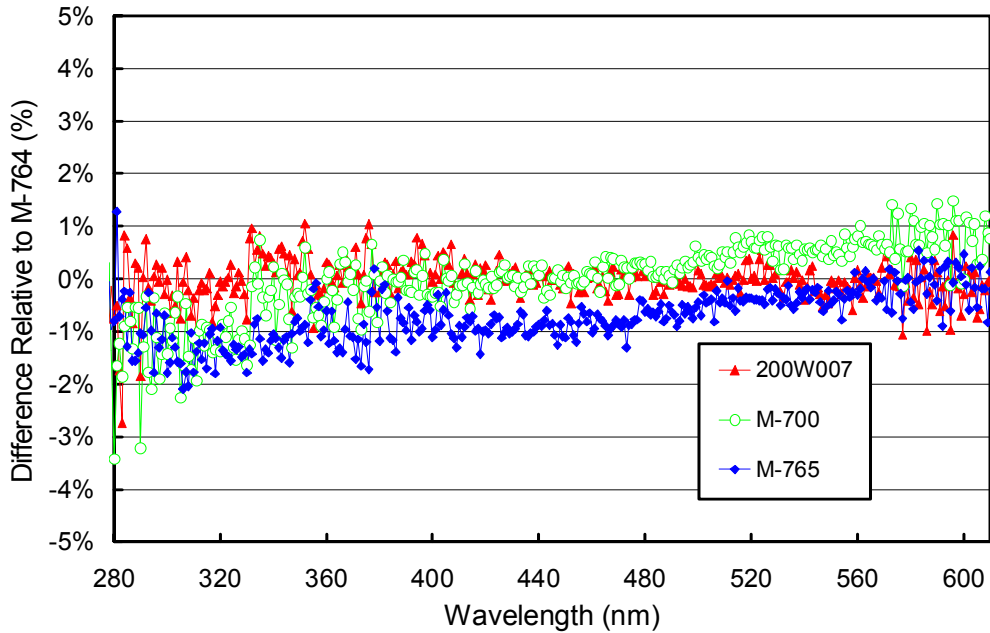


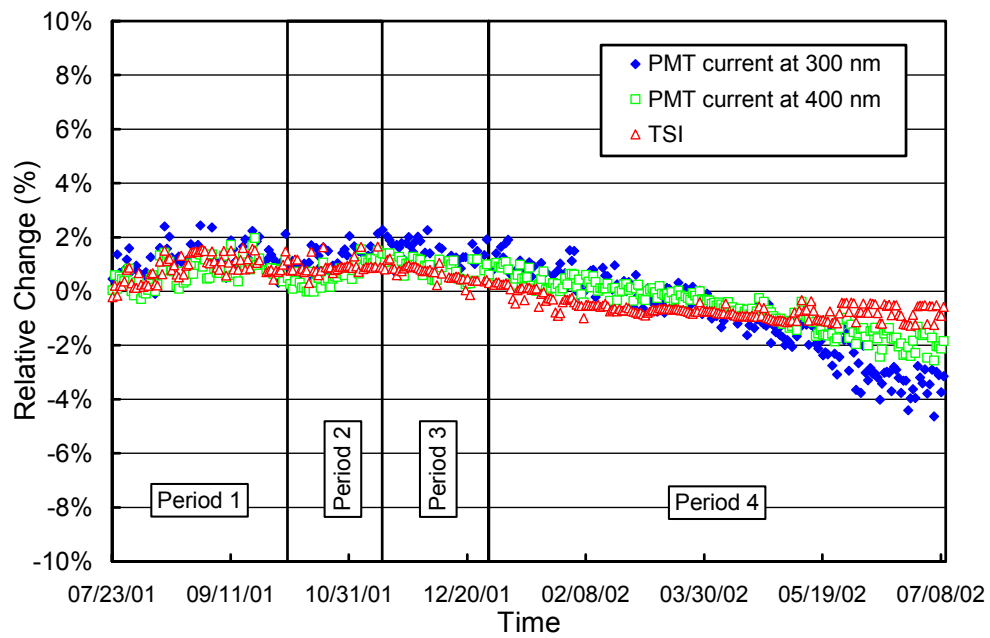
**Figure 5.2.2.** Comparison of Palmer lamps 200W007, M-700, and M-765 with the BSI traveling standard M-764 at the end of the season (7/10/02).

### 5.2.2. Instrument Stability

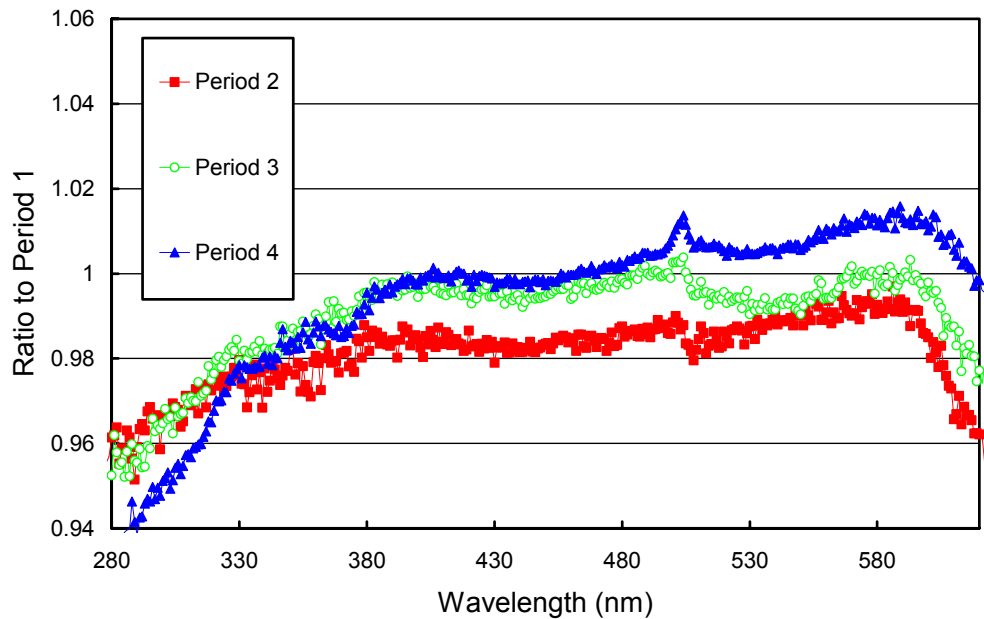
The stability of the spectroradiometer over time is primarily monitored with bi-weekly calibrations utilizing the site irradiance standards and daily response scans of the internal irradiance reference. The stability of the internal lamp itself is monitored with the TSI sensor, which is independent from possible monochromator and PMT drifts. By logging the PMT currents at several wavelengths during response scans, changes in the instrument responsivity can be detected.

Figure 5.2.3 shows the changes in TSI readings and PMT currents at 300 and 400 nm, derived from the daily response scans of the Palmer 2001/02 season. The TSI measurements indicate that the internal lamp was stable to within  $\pm 1.5\%$ ; PMT currents were stable to within  $\pm 3\%$ , and track the TSI measurements well.

Although analysis of the response scans suggested good stability of the system, calibrations with 200-Watt lamps suggested that the radiometric accuracy of the instrument can be improved by breaking the season into four periods with different absolute calibrations applied in each period. Figure 5.2.4 shows the ratio of these spectra, referenced to the first spectrum. The relative change from one spectrum to the next is generally smaller than 2%, except for wavelengths below 330 nm between Period 1 and 2. In addition, the standard deviation of the individual spectra contributing to the average spectrum for each period were calculated. Figure 5.2.5 shows the ratio of the standard deviation and average spectra. The ratios are useful for estimating the variability of the calibrations in each period. Figure 5.2.5 shows that the standard deviation is usually less than 1% of the average for all periods in the UV-A and visible, and increases slightly towards shorter wavelengths. Thus the calibrations in all periods are consistent to the  $\pm 1\%$  ( $\pm 1\sigma$ ) level.



**Figure 5.2.3.** Time-series of PMT current at 300 and 400 nm, and TSI signal during measurements of the response lamp during the Palmer 2000/01 season. The data is normalized to the average of all periods.



**Figure 5.2.4.** Ratios of irradiances assigned to the internal reference lamp compared to Period 1.

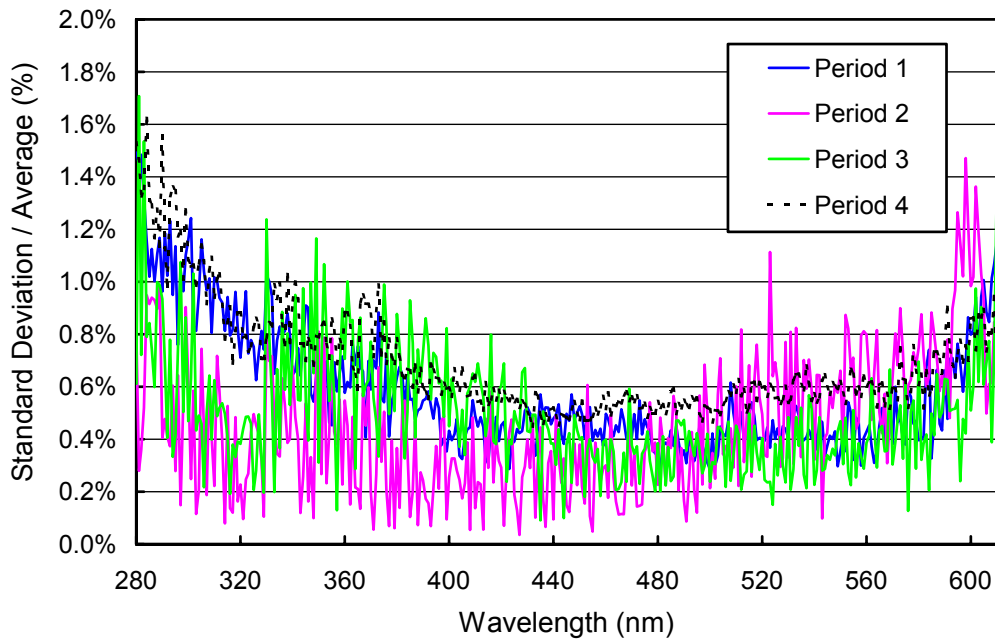


**Figure 5.2.5.** Ratio of standard deviation and average calculated from the absolute calibration scans.

### 5.2.3. Wavelength Calibration

Wavelength stability of the system was monitored with the internal mercury lamp. Information from the daily wavelength scans was used to homogenize the data set by correcting day-to-day fluctuations in the

wavelength offset. After this step, there may still be a deviation from the correct wavelength scale, but this bias should ideally be the same for all days. Figure 5.2.6 shows the differences in the wavelength offset of the 296.73 nm mercury line between two consecutive wavelength scans. In total, 368 scans were evaluated. For 98% of the days, the change in offset was smaller than  $\pm 0.015$  nm; for 99% of the days the shift was smaller than  $\pm 0.035$  nm. The excellent wavelength stability can partly be attributed to the new peak finding algorithm, which was first implemented for Palmer Volume 11 data. It is based on a Gaussian line fit, which leads to an improved accuracy compared to the tangent method that was used previously. See Section 4 for details. Figure 5.2.6 indicates that there are four occasions when the offset-difference was larger than  $\pm 0.1$  nm because the system lost its wavelength position and had to be re-initialized. The published data were appropriately adjusted.

After the data was corrected for day-to-day wavelength fluctuations, the wavelength-dependent bias between this homogenized data set and the correct wavelength scale was determined with the Fraunhofer-correlation method, as described in Section 4. Two correction functions were applied and are shown in Figure 5.2.7. One function was used between 7/23/01 and 9/24/01 (“Part 1”), and between 12/10/01 and 7/11/01 (“Part 3”). The second function was used between both periods, from 9/25/01 to 12/09/01 (“Part 2”). Immediately before Part 2, the system lost its wavelength position and had to be manually reset. The same problem occurred again at the end of Part 2. Adjustment of the wavelength offset usually does not modify the monochromator wavelength mapping. Our analysis of Palmer data indicates, however, that it changed after the first offset adjustment. In particular wavelengths between 300 and 340 nm and around 410 nm are affected. It is therefore likely that some resistance within the monochromator drive train caused the system to lose its position, and also led to the modified mapping function. The problem disappeared after the second offset adjustment on 12/10/01. The mapping function of Part 1 was therefore also applied to Part 3. The position was lost two more times, on 12/26/01 and 12/30/01, but the mapping did not change significantly. An inspection of the monochromator during the site visit in 2002 did not indicate the source of the problem.

After the data was wavelength corrected using the two functions described above, the wavelength accuracy was tested again with the Fraunhofer method. The results are shown in Figure 5.2.8 for four UV wavelengths. The residual shifts are generally smaller than  $\pm 0.05$  nm. The variation is slightly higher during Part 2, pointing again to increased resistance in the monochromator drive. There is more scatter at 310 nm during June and July because of the small solar irradiance levels that prevail during this part of the year, which affect the correlation algorithm.

Although data from the external mercury scans do not have a direct influence on the data products, they are part of our instrument characterization routine. Figure 5.2.9 illustrates the difference between internal and external mercury scans collected during both site visits. The wavelength scale of the figure is the same as applied during solar measurements. External scans have a bandwidth of about 0.93 nm FWHM; the bandwidth of the internal scan is only 0.73 nm. Internal scans of both periods are shifted by about 0.06 nm to shorter wavelength with respect to their external counterparts. Since external scans have the same light path as solar measurements, they more realistically represent the monochromator bandpass relevant for solar scans.

#### 5.2.4. Missing Data

As mentioned in the introduction, no solar data is available between 5/18/01 (end of Volume 10) and 7/22/01 (start of Volume 11) due to scheduled system service. A total of 18430 scans are part of the published Palmer Volume 11 data set. These are 96% of all scans scheduled. Of the missing scans, 94, 86, and 109 were superseded by absolute, wavelength, and response scans, respectively. Since Palmer Station has almost 24 hours of sunlight per day in December, a loss of data scans cannot be avoided. The system lost the wavelength position four times during the Volume 11 period. Following days are affected; numbers in parentheses give number of lost spectra: 9/22/01 – 9/25/01 (181); 12/9/01 – 12/11/01 (161); 12/25/01 – 12/26/01 (164); and 12/29/01 – 12/30/01 (63).

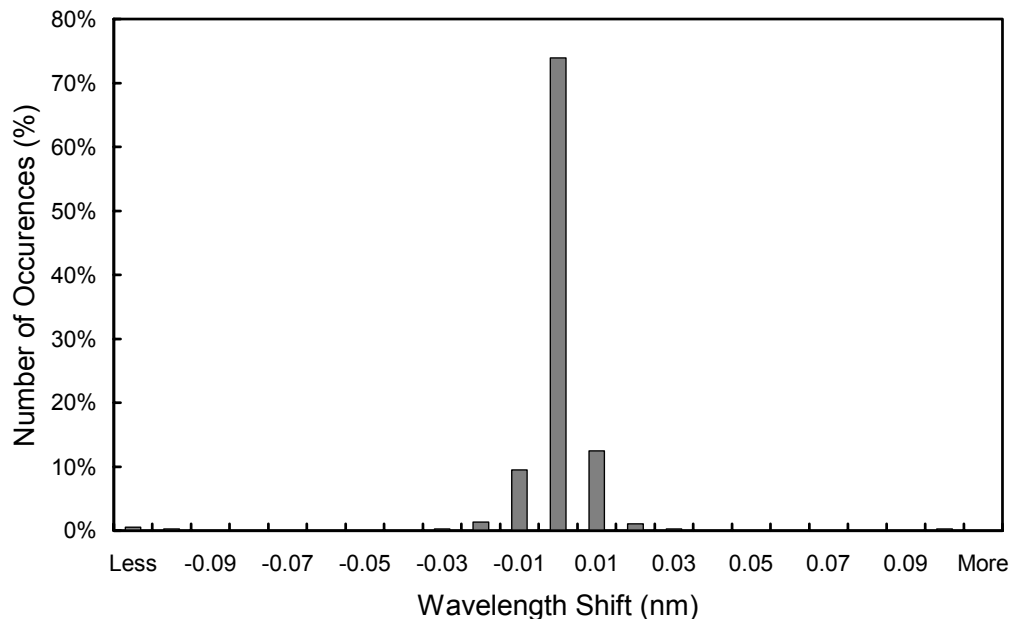


**Figure 5.2.6.** Differences in the measured position of the 296.73 nm mercury line between consecutive wavelength scans. The x-labels give the center wavelength shift for each column. Thus the 0-nm histogram column covers the range -0.005 to +0.005 nm. “Less” means shifts smaller than -0.105 nm; “more” means shifts larger than 0.105 nm. The excellent wavelength stability can partly be attributed to the new Gaussian peak finding algorithm, which was first implemented for Palmer Volume 11 data.

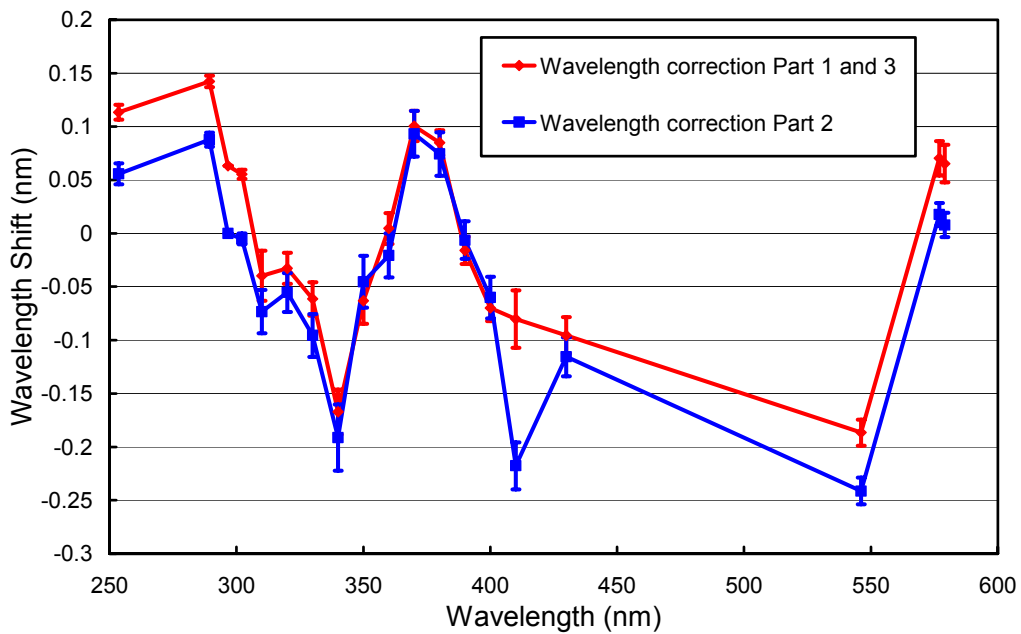


**Figure 5.2.7.** Monochromator mapping functions for the Palmer 2001/02 season. Part 1 refers to the period 7/23/01 – 9/25/01, Part 2 to the period 9/26/01 – 12/9/01, and Part 3 to 12/10/01 – 7/11/01.

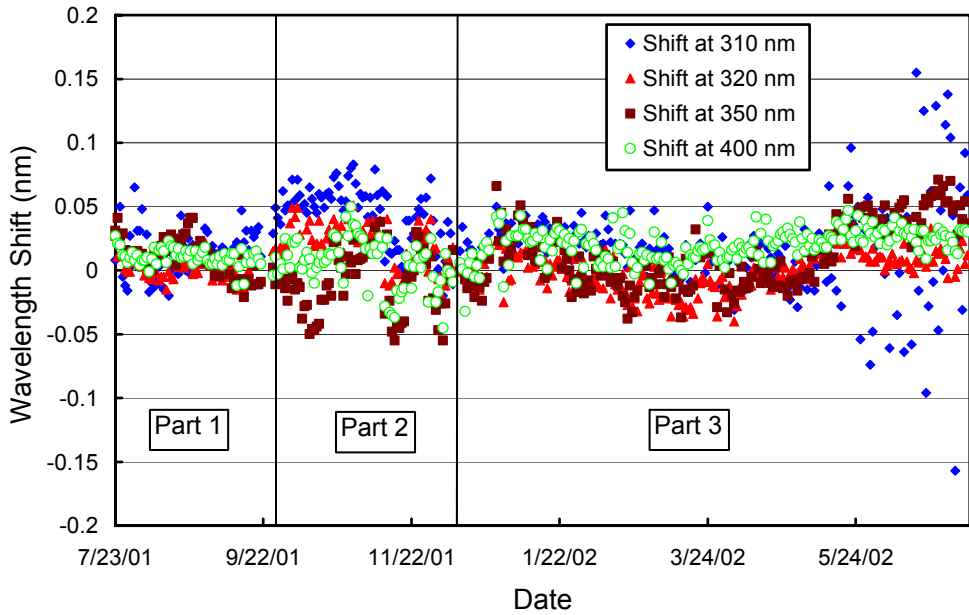


**Figure 5.2.8.** Wavelength accuracy check of the final data at four wavelengths by means of Fraunhofer correlation. The noontime measurement has been evaluated for each day of the season.

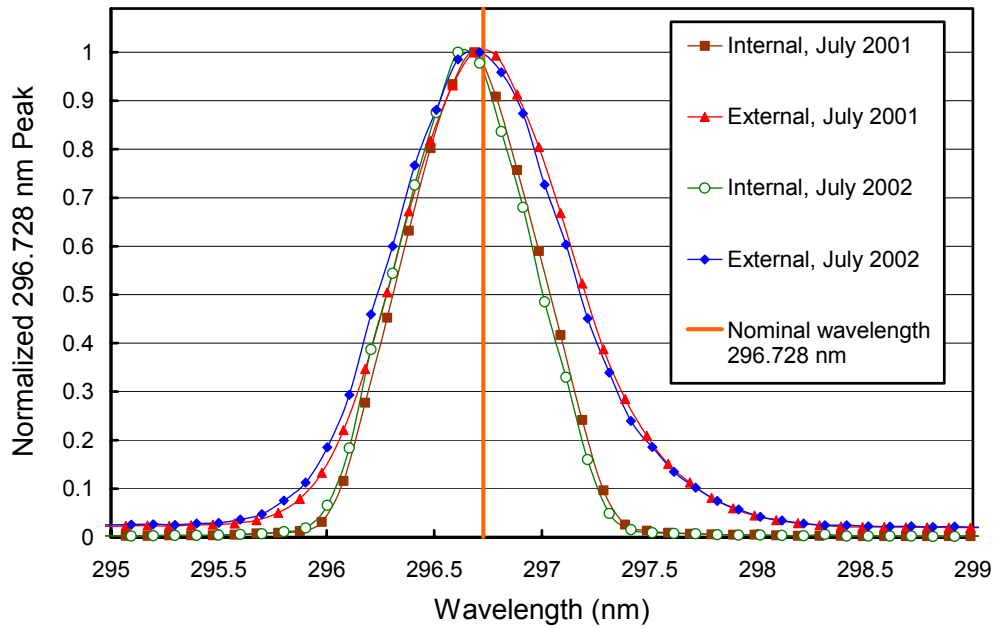


**Figure 5.2.9.** The 296.73 mercury line as registered by the PMT from external and internal sources. The wavelength scale is the same as applied for solar measurements.